Angewandte Chemie
Eine Zeitschrift der Gesellschaft Deutscher Chemiker

Supporting Information

69451 Weinheim, Germany

The Largest Synthetic Structure with Molecular Precision: Towards a Molecular Object**

*Baozhong Zhang, Roger Wepf, Karl Fischer, Manfred Schmidt, Sébastien Besse, Peter Lindner, Benjamin T. King, Reinhard Sigel, Peter Schurtenberger, Yeshayahu Talmon, Yi Ding, Martin Kröger, Avraham Halperin, and A. Dieter Schlüter**

anie_201005164_sm_miscellaneous_information.pdf

Table of Contents

1. Materials

TMV: Rothamsted common TMV strain kindly provided by B. Kassanis

Purification:

TMV infected leaves from *Nicotiana clevelandii* Grey were collected 10 days after inoculation and stored frozen until virus extraction. Frozen leaves (100 g) were thawed, homogenized in 0.2 % thioglycollic acid containing 0.18 M citric acid/ phosphate buffer (CP-buffer) pH 7 (300 mL) and filtered. The filtrate was pooled with an equal volume of chloroform and was shaken for 5 min. The upper clear phase was collected after low speed centrifugation (20 min at 3300 g) and submitted to two cycles of differential centrifugation (60 min at 125000 g and 10 min at 10000 g). Virus containing pellets were resuspended in 0.018 M CP-buffer pH 7 (10 mL). The process was repeated using less (1 mL) buffer. The virus nucleoprotein was further purified by sucrose density gradient centrifugation (linear gradient made of 10 to 40 % sucrose (w/v) in 0.018 M CP-buffer pH 7 in 35 mL tubes and centrifuged for 150 min at 25'000 rpm in a SW 32 Ti rotor). The gradient was fractionated to ~1.6 mL fractions whereby the presence of virus particles was monitored by UV absorption spectrophotometry. Excess of sucrose was removed by sedimentation of virus particles (150 min at 125000 g) and resuspension of the pellet in 0.018 M CP-buffer pH 7.

2. Methods

2.1. Atomic force microscopy

AFM measurements were carried out on a Nanoscope® IIIa Multi Mode Scanning probe microscope (from Digital Instruments, San Diego, CA) operated in the tapping mode with an "E" scanner (scan range 10 μm x10 μm) and operated in the tapping mode at room temperature in air. Olympus silicon OMCL-AC160TS cantilevers (from Atomic Force F&E GmbH, Mannheim,

Germany) were used with a resonance frequency between 200 and 400 kHz and a spring constant around 42 N/m. The samples were prepared by spin-coating (2000 rpm) the polymer solution (3-4 mg/L chloroform) onto freshly cleaved mica (from PLANO W. Plannet GmbH, Wetzlar, Germany).

2.2. Light scattering

Static light scattering measurements were performed either with an ALV-SP86 goniometer, an Uniphase HeNe laser (25 mW output power at 632.8 nm wave length), or an ALV/High QE APD avalanche diode fiberoptic detection system. Dynamic light scattering was measured with an ALV-7000 instrument operating simultaneously with eight detectors (ALV/High QE APD avalanche diode fiberoptic detection systems) at eight different scattering angles (30 to 150 degrees) and eight correlators. The static scattering intensities were measured from 30^o to 150^o in steps of 5^o and analyzed according to standard procedures in terms of Zimm-plots yielding the weight average molar mass, M_w, the mean square radius of gyration, $R_g^2 = \langle R_g^2 \rangle_z$, and the second virial coefficient, A_2. The correlation functions were analyzed by a second order cumulant or a biexponential fit. The z-average diffusion coefficient D_z was obtained by extrapolation of the reduced initial slope Γ/q^2 for to q = 0. The inverse z-average hydrodynamic radius $R_h = \langle 1/R_h \rangle_z^{-1}$ was evaluated by formal application of Stokes law. The polymers were dissolved in methanol plus 10^{-3} M LiBr (**$PG1_{long}$ -$PG5_{long}$:** $0.08 \leq c \leq 0.025$ mg/mL) and filtered (Millex GHP, 200 nm pore size) into dust-free Suprasil cuvettes (Hellma, 20 mm diameter). No concentration losses could be detected for **$PG1_{long}$** by comparing the count rates of filtered and unfiltered solutions, respectively. For **$PG4_{long}$** filtration was not possible due to large concentration losses upon filtration through even 800 nm pore size filters. Therefore, **$PG4_{long}$** was dissolved at a high concentration of 1 g/L. Three drops of the unfiltered solution were added to a Suprasil cuvette containing a large excess of filtered methanol/LiBr, yielding a final concentration of c = 7.63 mg/L. Since such a small

concentration effectively represents the infinite dilution limit, no further dilution was performed with **PG4$_{long}$**. Unfortunately, this procedure could not be applied to **PG5$_{long}$** because the sample was contaminated with larger dust particles which rendered a reliable light scattering measurement impossible. The refractive index increments were measured by a home built Michelson interferometer as described elsewhere[1] and determined to dn/dc = 0.1732 for **PG1$_{long}$** and dn/dc = 0.1943 cm^3/g for **PG4$_{long}$**.

2.3. Small-Angle Neutron Scattering

Small angle neutron scattering (SANS) was performed at the instrument D11 of the Institute Laue Langevin. With a neutron wavelength of 0.6 nm and 3 sample detector distances (1.2 m, 8 m, 20 m), a range 0.03-5 nm^{-1} of scattering vectors q was covered. **PG5$_{short}$** was dissolved in deuterated methanol and measured in cells of 2 mm thickness at several concentrations (0.09-3.6 wt-%). The chain cross section is extracted from high q SANS data, where the form factor becomes equivalent to the scattering of a rod like particle with finite thickness. Interaction effects are absent in this range, so a concentration extrapolation is not required. A first estimate for the chain cross section R_{box}= 5.0 nm is obtained from a cross section Guinier plot. In this simple model, R_{box} represents the radius of a rod with homogeneous density. A more detailed analysis is based on the indirect Fourier transform and a convolution square-root technique,[2] which is available in the software packages GIFT and DECON. The model free analysis reproduces also the oscillations in the SANS data at high q and yields the cross section profile of a rod like particle. Figure 4 displays the normalized cross section profile, which compares well with R_{box} and R_{vdW}. The persistence length L_p=30 nm is obtained from a fit of the Kholodenko from factor,[3] where a log-normal distribution is assumed for the chain length.

2.4. TEM, SEM

For height measurements **PG5** was either absorbed by spin coating onto freshly cleaved mica (PLANO W. Plannet GmbH, Wetzlar, Germany) or onto HOPG (SPI Supplies, Westchester, PA, USA) These air dried samples were mounted under liquid nitrogen onto a cryo-SEM stage and transferred from liquid nitrogen into a freeze-etching device (BAF400 Bal-Tec/Leica, Vienna) and shadowed with 1.5 nm W from an elevation angle of 7° at -80°C.

For TEM these shadowed samples were additionally coated with a 5-8 nm layer of carbon to stabilize the metal film for replica production. The samples were then withdrawn from the high vacuum chamber and the metal-carbon replica on mica was floated onto a clean water surface. Floating pieces of the replica were then loaded onto 400 mesh glow discharged Cu-TEM grids (PLANO W. Plannet GmbH, Wetzlar, Germany) and dried in air prior to TEM investigation in a CM12 (FEI, Netherlands) at 100 kV. Images were recorded digitally with a Gatan Orius CCD camera.

For HR-SEM width investigations **PG5** samples were passively adsorbed from a 3 µl drop of liquid on glow discharged carbon coated (4 nm) Cu-grid (PLANO W. Plannet GmbH, Wetzlar, Germany) for 30 second. After blotting off any excess liquid the grids were plunge frozen in liquid nitrogen. The still frozen samples were then freeze dried at -80°C under high vacuum ($<5*10^{-7}$ mbar) for 2 h followed by metal coating with 2.5 nm W in a freeze etching device BAF400 (Bal-Tec, Balzers, Lichtenstein). To preserve the three-dimensional structure, samples were always kept below -80°C and transferred under high vacuum (VCT-100, Bal-Tec) to a cryo-FE-SEM (Gemini 1530, Zeiss, Germany) at -120°C and loaded onto the pre-cooled cryo-stage (-120°C). Imaging was performed at -120°C simultaneously in the SE and BSE mode at acceleration voltages of 2-10kV and digitally recorded.

2.5. Cryo-TEM

Vitrified specimens for electron microscopy were prepared in a controlled environment vitrification system (CEVS) at 25 ºC, as previously described.[4] In brief, a drop of the examined solution was applied onto a perforated carbon film, supported on an electron microscopy copper grid, held by the CEVS tweezers. The sample was blotted and immediately plunged into liquid nitrogen (-196 °C). Note that the cryogen of choice, liquid ethane at its freezing point, cannot be used in this case, as it dissolves dioxane. However, liquid nitrogen is a sufficiently effective cryogen to vitrify dioxane, as well as many other organic solvents.[5] The vitrified samples were then stored under liquid nitrogen, and later examined in an FEI T12 microscope operated at 120 kV. A Gatan 626 cooling holder system was used to transfer specimens into the microscope. Images were recorded in the low-dose mode, to minimize electron-beam radiation-damage to the radiation-sensitive samples. We used a Gatan US1000, high-resolution cooled CCD camera to record the images, at nominal underfocus of 1-2 μm to enhance phase contrast.

2.6. Simulation

For the simulated density profile $\rho_n(r)$ shown in Fig. 4b, **PG5** with $P_n = 250$ dendrons attached to each second atom of a freely rotating backbone (bond length 1.54 Å, spatial distance 2.5 Å between repeat units) has been modelled by a united atom (UA) model which fully captures the **PG5** topology. The model neglects chemical structures such as aromatic rings and amide conductivities of relevance for length scales below a typical distance between adjacent branching points, accordingly, dihedral hindrances are not taken into account. UAs are interacting via the repulsive part of a Lennard-Jones (LJ) potential (resembling good solvent quality), bond length is approximately kept fixed during a brownian dynamics simulation run, terminal UAs are charged and interact electrostatically (for remaining details see Ref. 6). The initial configuration has been prepared via Monte Carlo, where UAs are treated as hard spheres and grown starting from a self-avoiding, freely rotating backbone. The dendron model employed here has $s = 7$ spacer UAs

between adjacent junctions, $\sum_{g=1}^{G}(2^g(s+1)+2^{g-1}) = 17\times 2^G - 7 = 527$ UAs per single dendron. A single UA has a mass of 20.4 Da, van der Waals volume corresponding to 28 $Å^3$, the fully stretched dendron (strand) has an end-to-end distance of 5.9 nm. The **PG5** conformation with about 131,750 UAs and 8,000 counterions has been followed in time for a duration of multiple relaxation times (300,000 LJ units during one week on a single graphics card with 256 processors). The radial density profile $\rho_n(r)$, normalized as $1 = 2\pi\int r\rho_n(r)dr$ has been obtained by first constructing the centreline of the dendronized polymer (cf. Ref. 6), and subsequent calculation of shortest distances between all UAs and the centreline. We measured a value 0.77 ± 0.08 for the ratio between apparent length and maximal extension of the backbone, in accord with a radial density profile which does not exactly vanish at distances exceeding the size of the maximally stretched dendron.

*2.7. Synthetic procedures for de-**PG4**$_{long}$ and **PG5**$_{long}$*

Synthesis of *de*-**PG4**$_{long}$: To a well-stirred, freeze-dried powder of **PG4**$_{long}$ (0.10 g, 0.018 mmol) in a round bottom flask was added dropwise trifluoroacetic acid (TFA) (3 mL) and methanol (0.1 mL) at room temperature. After all solid materials were dissolved, the mixture was stirred at room temperature for 6 days. Afterwards, methanol (10 mL) was added and the mixture then evaporated. The same methanol addition and evaporation procedure was repeated three times, before the residue was dissolved in water (15 mL) and carefully lyophilized from dioxane (200 mL) to yield a powdery white solid as the product *de*-**PG4**$_{long}$ as the trifluoroacetate (0.10 g, 100%). ^{1}H NMR (500 MHz, DMF-d_7): δ = 0.92 (br, 2 H, CH_3), 1.34 (br, 5 H, CH_3), 1.99-2.18 (br, 60 H, CH_2), 3.20-3.47 (br, 60 H, CH_2NH), 4.08 (br, 60 H, CH_2O), 6.54-6.62 (br, 18 H, Ph), 7.05 (br, 26 H, Ph), 8.37 (br, 33 H, Ph, NH). The NMR spectrum is shown in Figure S1

Synthesis of **PG5**$_{long}$: In a typical growth step, triethylamine (47 mg, 0.46 mmol) and the acylation catalyst *N*,*N*-dimethylaminopyridine (DMAP) (47 mg, 0.08 mmol) were added to a

dimethylformide (DMF) solution (170 mL) of *de*-**PG4$_{long}$** (0.0184 mmol) at −5 °C. A solution of dendron active ester **1** (1.040 g, 1.84 mmol) in 20 mL DMF was added in six portions over 20 days. During the addition of each portion, the reaction mixture was cooled to −10 °C, then slowly warmed to rt and stirred for 2-3 days. Thereafter the reaction mixture was concentrated *in vacuo* and the residue dissolved in 20 mL of dichloromethane followed by column chromatographic purification (eluent: dichloromethane, R_f = 0.1). This furnished a beige gel, which was freeze-dried from 1,4-dioxane (40 mL) to yield **PG5$_{long}$** as a powdery, slightly off-white solid (86 mg, 42%). ^{1}H NMR (500 MHz, DMF-d_7): δ = 1.36 (br, 288 H, CH_3), 1.87 (br, 86 H, CH_2), 3.05 (br, 54 H, CH_2), 3.17 (br, 54 H, CH_2), 3.62 (br, 32 H, CH_2), 3.98 (br, 58 H, CH_2), 6.15 (br, 32 H, CH), 6.55 (br, 26 H, CH), 6.99 (br, 32 H, CH), 8.16 (br, 2 H, NH). The NMR spectrum is shown in Figure S1.

The same procedure was applied to **PG4$_{short}$** (0.38 g) to give 0.46 g of **PG5$_{short}$** (62%). Anal. Calcd for $(C_{567}H_{822}N_{62}O_{158})_n$: C, 61.73: H, 7.54; N, 7.74. Found: C, 61.47; H, 7.19; N, 7.50.

It is assumed that the mass loss, amounting to 58% for **PG5$_{long}$** and 38% for **PG5$_{short}$** is due to polymer remaining on the column. While it is possible that the purification procedure fractionated the polymer, with the longer chains are preferentially retained on the column, this does not seem to be the case. Large scale SEM images of **PG5$_{long}$** (see Figure S4) show chains with contour lengths of a few micrometers.

2.8. Quantification of Dendronization

Sample preparation: The UV-labelled **PG5** was prepared by a procedure that was reported earlier.[7] To a well-stirred solution of dendronized polymer **PG5** (15 mg) in 1,1,2,2-tetrachloroethane (0.2 mL) was added 0.1 M $NaHCO_3$ solution (0.26 mL) and a solution of Sanger's reagent (2.4 mg, 0.3 eq. per amino group) in 1,1,2,2-tetrachloroethane (0.3 mL). The

reaction mixture was heated with stirring at 65 °C for 3 h. After cooling to rt, 1,1,2,2-tetrachloroethane (2 mL), water (2 mL) and citric acid (1 mg) were added. The separated organic layer was washed with water (1 mL) and brine (1mL), concentrated *in vacuo*, re-dissolved in THF (1 mL) and precipitated into methanol/water (4:1). The same procedure was performed four times to yield 2,4-dinitroaniline-labeled **PG5** (13 mg, 87%) as a yellowish solid.

Measurements: The quantitative UV experiments were performed on Perkin Elmer Lambda 20 UV/vis spectrometer by using 1 mm quartz cuvettes. The UV-labelled **PG5** was dissolved in 1,1,2,2-tetrachloroethane with a concentration of 5.41×10^{-5} mol/L (repeat unit). The extinction coefficient (ε) of 2,4-dinitroaniline moiety follows the value of reference compound **1** (Figure S2) as 1.64×10^{4} $Lmol^{-1}cm^{-1}$.[7] The concentration of the dinitroanilino moieties, which is also considered as the concentration of unconverted terminal amino groups (supposing all the unreacted amino groups in the dendronization were labelled by treating with Sanger's reagent), was calculated according to Lambert-Beer law ($c=A/\varepsilon l$). In this equation, l denotes the inside width of the UV cuvettes (0.1 cm) and A denotes the maximum absorption at 357 nm. The structure perfection X for the conversion from ***de*-PG4** to **PG5** was therefore calculated as $X = (1-c/c^{0}) \times 100\%$, in which c denotes the concentration of 2,4-dinitroanilino moieties, and c^{0} denotes the concentration of total termini in the starting material (***de*-PG4**), which is 16 times of the molar concentration of **PG5** . The concern about the justification of applying the extinction coefficient of model compound **1** for structure perfection determinations has been addressed in the earlier reports.[7] The UV-vis spectra of **PG5** before and after UV-labelling are shown in Figure S3. From the absorption of labelled **PG5** at 357 nm, the degree of coverage of **PG5** (or the perfection of the dendronization) was calculated as 97.1%, and if corrected for the almost negligible absorption of unlabeled **PG5** at 357 nm, the perfection was 97.5%.

3. Supplementary Discussion

3.1. Light scattering

Multi angle laser light scattering measurements of methanol solutions of the starting polymer, **PG1$_{long}$**, resulted in a perfect Zimm plot from which M_w = 9.23 x 10^6 Da (P_w = 17 600) was extracted (Figure S4). This value is larger than the GPC value reported earlier.[8] The polydispersity index could be estimated by GPC to M_w / M_n = 2 and accordingly, P_n = 8 800 which translates into an average main chain contour length of ~2.2 μm assuming an all-trans conformation. The radius of gyration was determined to R_g = 96 nm, the hydrodynamic radius to R_h = 57 nm. Application of the wormlike chain model resulted in a Kuhn statistical segment length of l_k = 8.5 nm, assuming a Schulz-Flory chain length distribution. This is close to the chain stiffness determined previously on other first generation dendrons.[9] For the scattering data obtained for **PG4$_{long}$**, see Figure S5.

3.2. Cryo-TEM

The image in Figure 3 shows that the chains can clearly be discerned from one another and have a diameter of Ø = 7 nm. The discrepancy between the *cryo*-TEM measurement and those of the other techniques may be the result of imperfect TEM magnification calibration due to small differences in specimen height along the optical axis. That is a complicated issue: to reach accurately enough magnification calibration one needs a built-in size standard in the field of view. Also, when dealing with a more-or-less cylindrical object, the "thinness" of the aggregate edges, makes it hard to determine where an aggregate ends, as contrast goes down at the edges, thus giving an apparent smaller size than the real value. Note that the SANS measurements were performed in chloroform, while the *cryo*-TEM work was done in dioxane. The difference in solvent quality may also contribute to the difference in the size measurements, by affecting the packing of the molecule in the solvent. The dioxane layer is approximately 100 nm thick, which should still allow the chains to be in a near native conformation.

4. Supplementary Figures

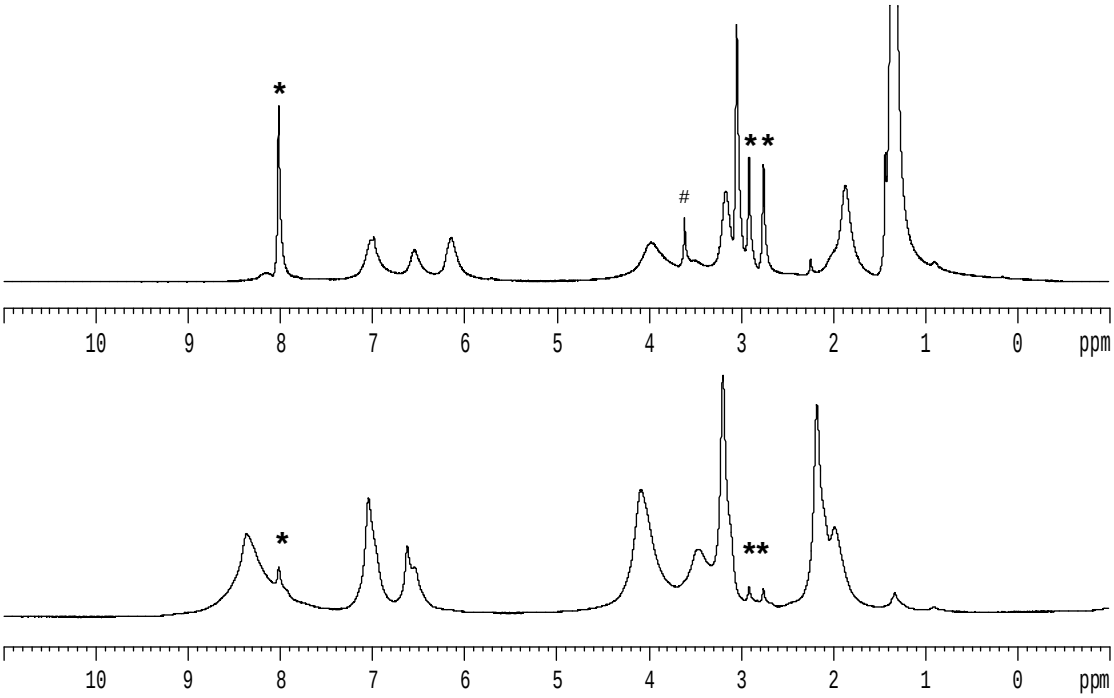

Figure S1 | ^{1}H NMR spectra of **PG5$_{long}$** (top) and *de*-**PG4$_{long}$** (bottom) in DMF-d_7 at 80 °C. The signals of the NMR solvent (*) and residual 1,4-dioxane (#) from freeze-drying are marked.

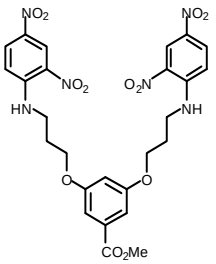

Figure S2 | Structure of reference compound **1**

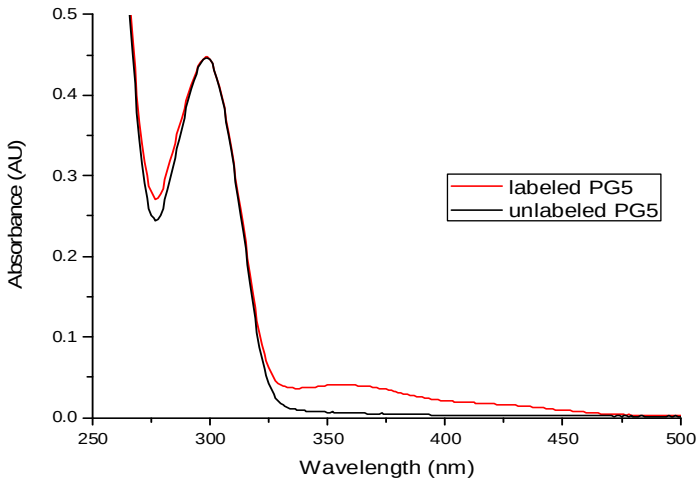

Figure S3 | UV-vis spectra of **PG5** before and after UV labelling

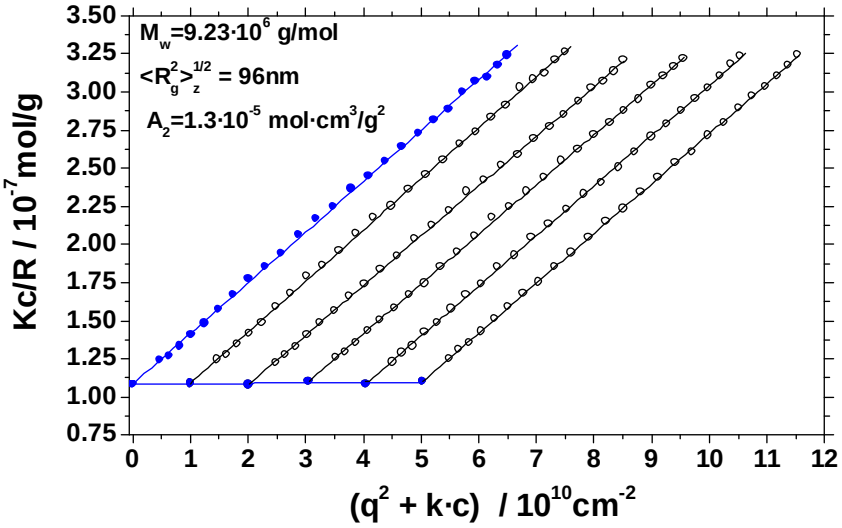

Figure S4 | Light scattering results for **PG1**$_{\mathbf{long}}$ in methanol.

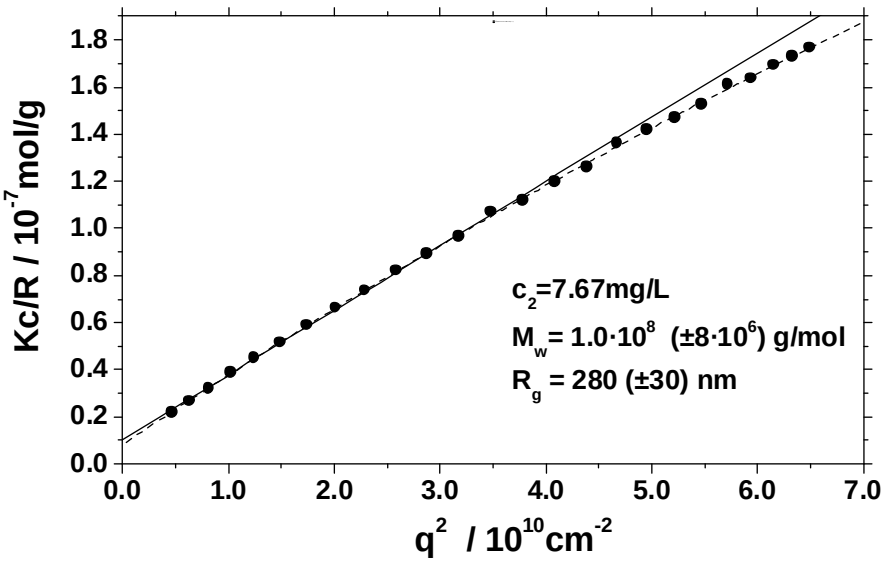

Figure S5 | Light scattering results for **PG4$_{long}$** in methanol.

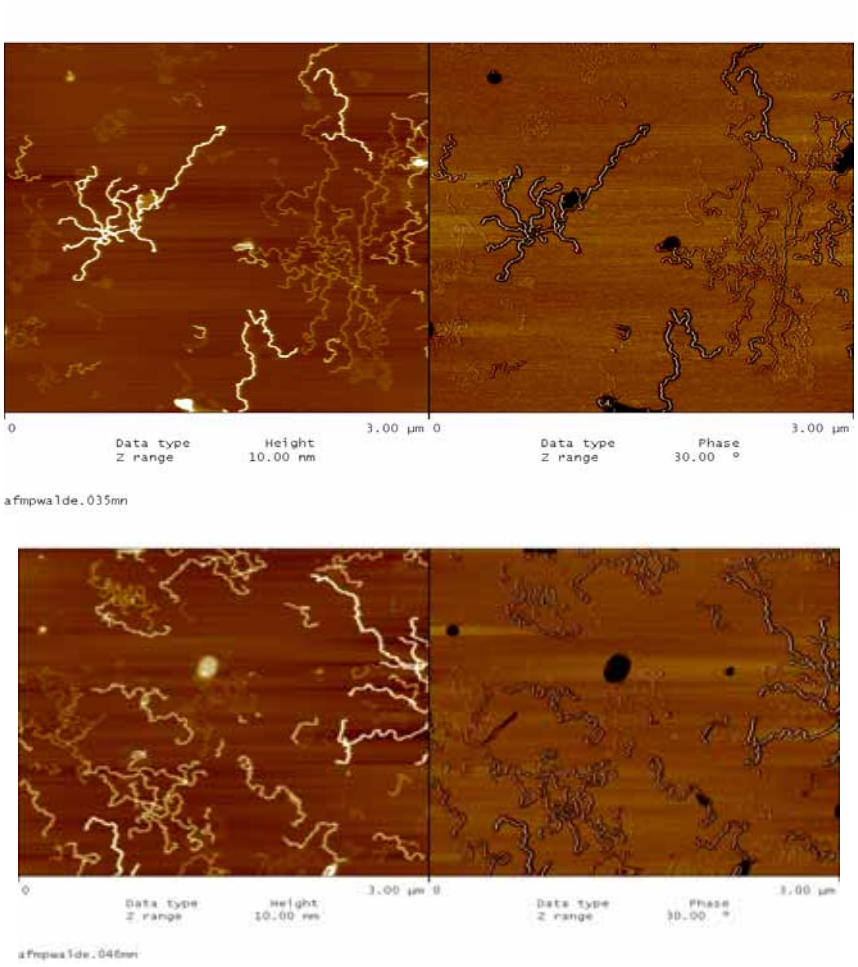

Figure S6 | Two large scale height (left) and phase contrast (right) AFM tapping mode images of co-prepared $\mathbf{PG1_{long}}$-$\mathbf{PG5_{long}}$ chains on mica under ambient conditions to illustrate that each individual chain can clearly be assigned to a particular generation.

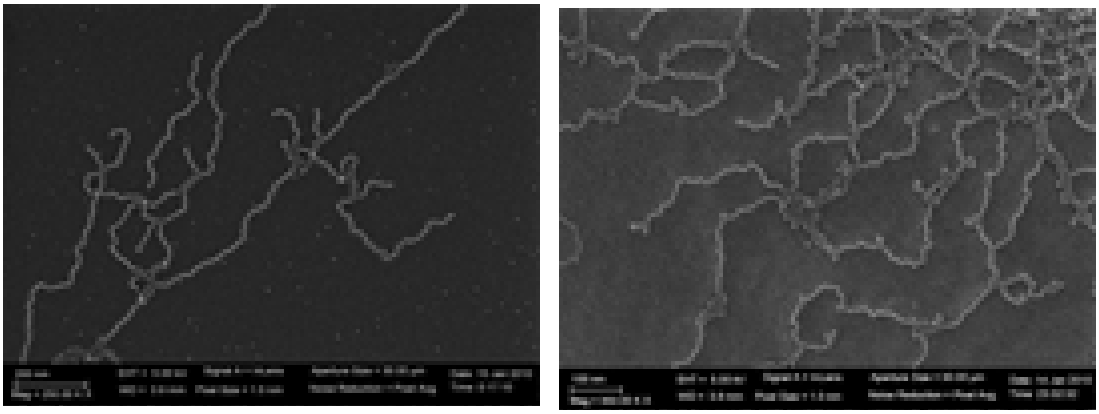

Figure S7 | Large scale rotary shadowed SEM images of **PG5$_{long}$** on amorphous carbon to illustrate the existence of very long chains supporting the argument that there is little fractionation associated with the column chromatographic purification step.

5. Supplementary References

1) Becker, A., Köhler, W., Müller. A Scanning Michelson Interferometer for the Measurement of the Concentration and Temperature Derivative of the Refractive Index of Liquids. Ber. Bunsenges. Phys. Chem. **99**, 600- (1995).

2) Glatter, O., Hainisch, B. Improvements in real-space deconvolution of small-angle scattering data J. Appl. Cryst. **17**, 435-441 (1984).

3) A. L. Kholodenko. Analytical calculation of the scattering function for polymers of arbitrary flexibility using the dirac propagator. Macromolecules **26**, 4179-4183 (1993).

4) Talmon, Y., Transmission electron microscopy of complex fluids: the state of the art, Ber. Bunsen-Ges. .Phys. Chem. **100**, 364-372 (1996).

5) Danino, D. Direct cryo-TEM imaging of phospholipid aggregates in soybean oil, J. Colloid Interface Sci. **249,** 180-186 (2002).

6) Ding, Y. et al. From atomistic simulation to the dynamics, structure and helical network formation of dendronized polymers: The Janus chain model, J. Chem. Phys. **127**, 094904 (2007).

7) Shu, L. et al. Quantitative aspects of the dendronization of dendronized linear polystyrenes. Macromol. Chem. Phys. **203**, 2540-2550 (2002).

8) Guo, Y., et al. Tuning polymer thickness: synthesis and scaling theory of homologous series of dendronized polymers. J. Am. Chem. Soc. **131**, 11841-11854 (2009).

9) Zhang, A., et al. Efficient synthesis of high molar mass. First- to fourth-generation distributed dendronized polymers by the macromonomer approach. Chem. Eur. J. **9**, 6083-6092 (2003).